# 1. Studies of signal and background separation using Mann-Whitney U test and some new methods

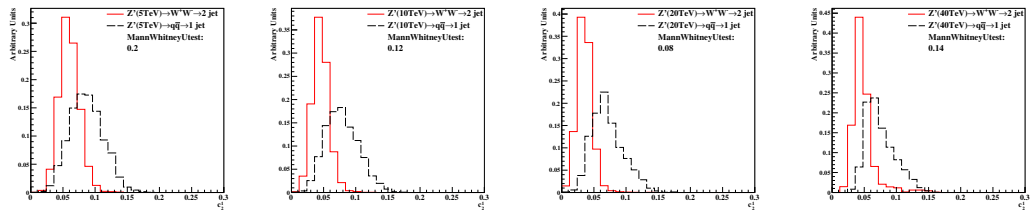


(a) 5TeV at 20×20(cm×cm) in cluster (b) 10TeV at 20×20(cm×cm) in cluster (c) 20TeV at 20×20(cm×cm) in cluster (d) 40TeV at 20×20(cm×cm) in cluster

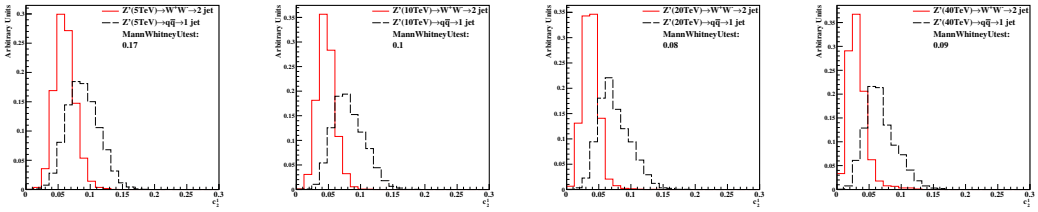


(e) 5TeV at 5×5(cm×cm) in cluster (f) 10TeV at 5×5(cm×cm) in cluster (g) 20TeV at 5×5(cm×cm) in cluster (h) 40TeV at 5×5(cm×cm) in cluster

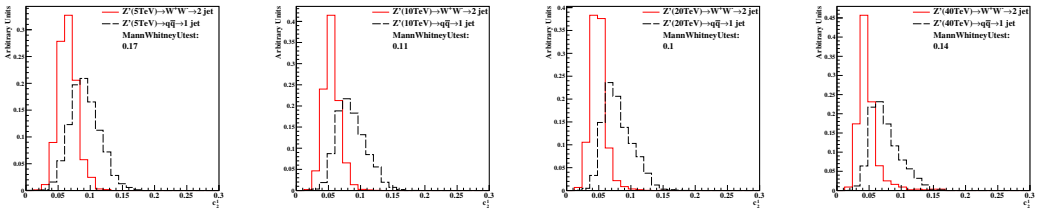


(i) 5TeV at 1×1(cm×cm) in cluster (j) 10TeV at 1×1(cm×cm) in cluster (k) 20TeV at 1×1(cm×cm) in cluster (l) 40TeV at 1×1(cm×cm) in cluster

Figure 1: Distributions of Mann-Whitney value U in 5,10,20,40TeV energy collision for $c_2^{(1)}$ in different detector sizes. Cell Size in 20×20, 5×5, and 1×1(cm×cm) are shown here.

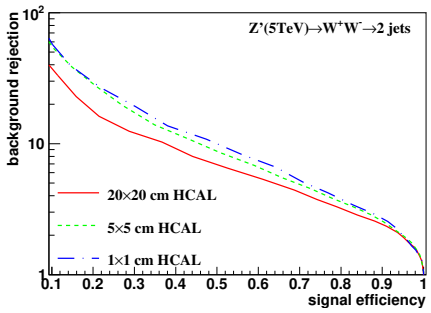


(a) 5 TeV in cluster

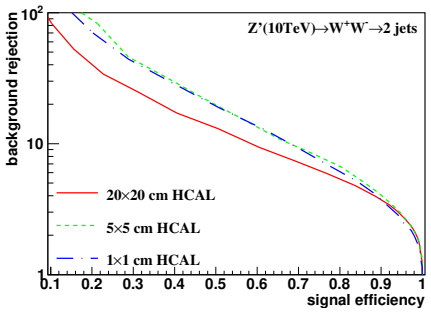


(b) 10 TeV in cluster

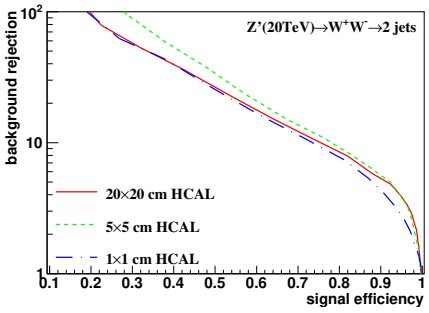


(c) 20 TeV in cluster

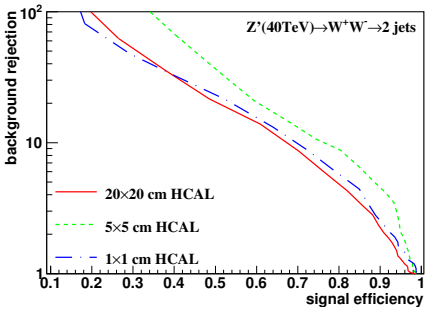


(d) 40 TeV in cluster

Figure 2: Signal efficiency versus background rejection rate using $c_2^{(1)}$.The energies of collision at (a)5, (b)10, (c)20, (d)40TeV are shown here. In each picture, the three ROC curves correspond to different detector sizes.

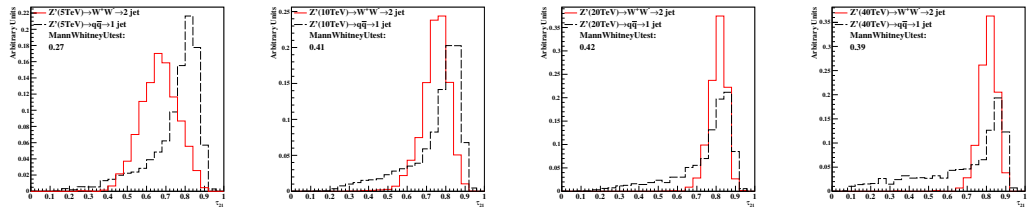


(a) 5TeV at 20×20(cm×cm) in 0.5GeV (b) 10TeV at 20×20(cm×cm) in 0.5GeV (c) 20TeV at 20×20(cm×cm) in 0.5GeV (d) 40TeV at 20×20(cm×cm) in 0.5GeV

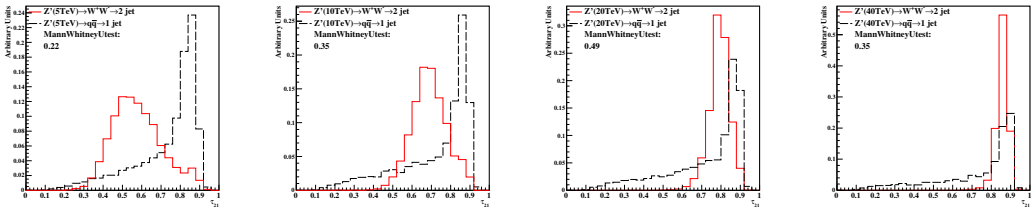


(e) 5TeV at 5×5(cm×cm) in 0.5GeV (f) 10TeV at 5×5(cm×cm) in 0.5GeV (g) 20TeV at 5×5(cm×cm) in 0.5GeV (h) 40TeV at 5×5(cm×cm) in 0.5GeV

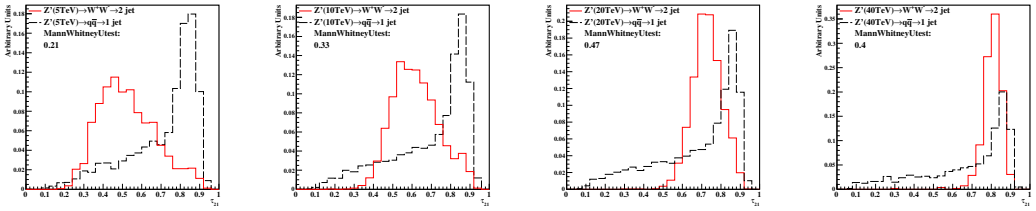


(i) 5TeV at 1×1(cm×cm) in 0.5GeV (j) 10TeV at 1×1(cm×cm) in 0.5GeV (k) 20TeV at 1×1(cm×cm) in 0.5GeV (l) 40TeV at 1×1(cm×cm) in 0.5GeV

Figure 3: Distributions of Mann-Whitney value U in 5, 10, 20, 40TeV energy collision for $\tau_{21}$ in different detector sizes. Cell Size in 20×20, 5×5, and 1×1(cm×cm) are shown here.

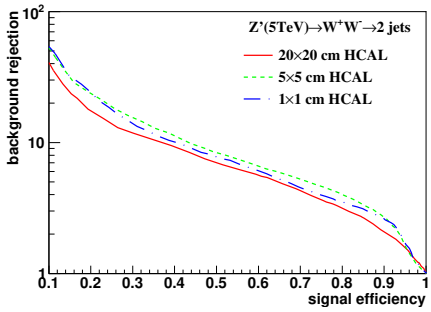


(a) 5 TeV rawhit cut at 0.5GeV compare with New2 Method

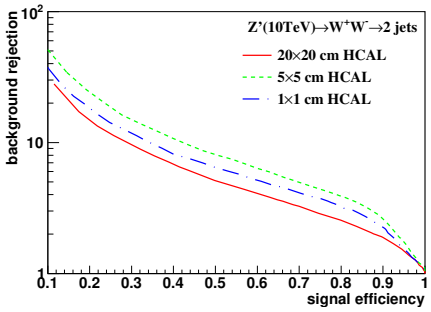


(b) 10 TeV rawhit cut at 0.5GeV compare with New2 Method

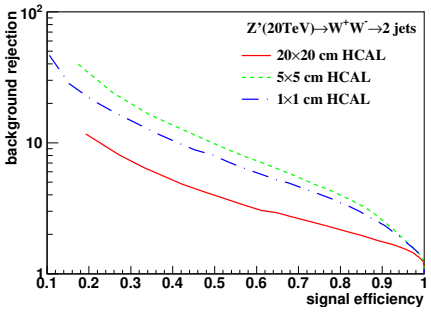


(c) 20 TeV rawhit cut at 0.5GeV compare with New2 Method

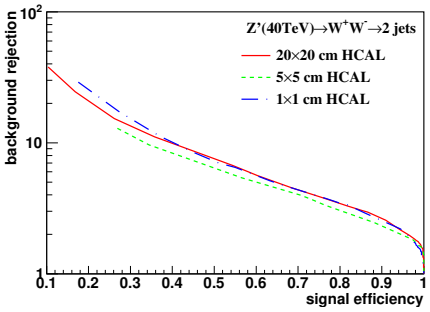


(d) 40 TeV rawhit cut at 0.5GeV compare with New2 Method

Figure 4: Signal efficiency versus background rejection rate using $\tau_{21}$.The energies of collision at (a)5, (b)10, (c)20, (d)40TeV are shown here. In each picture, the three ROC curves correspond to different detector sizes.

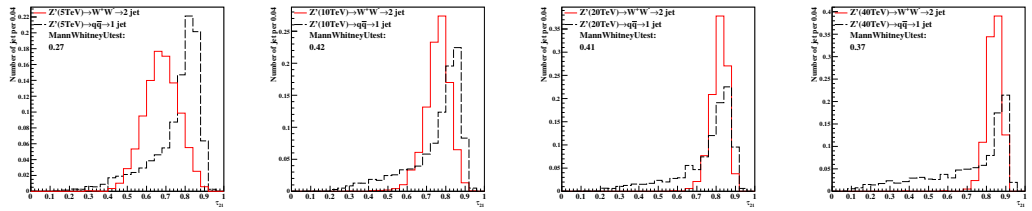


(a) 5TeV at 20×20(cm×cm) in 0.25GeV (b) 10TeV at 20×20(cm×cm) in 0.25GeV (c) 20TeV at 20×20(cm×cm) in 0.25GeV (d) 40TeV at 20×20(cm×cm) in 0.25GeV

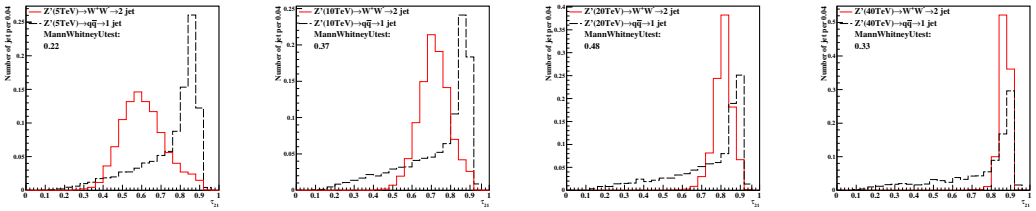


(e) 5TeV at 5×5(cm×cm) in 0.25GeV (f) 10TeV at 5×5(cm×cm) in 0.25GeV (g) 20TeV at 5×5(cm×cm) in 0.25GeV (h) 40TeV at 5×5(cm×cm) in 0.25GeV

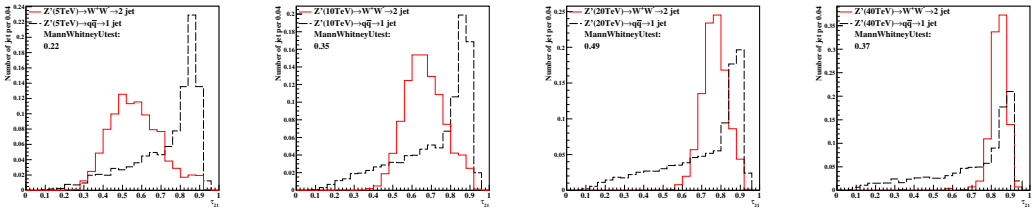


(i) 5TeV at 1×1(cm×cm) in 0.25GeV (j) 10TeV at 1×1(cm×cm) in 0.25GeV (k) 20TeV at 1×1(cm×cm) in 0.25GeV (l) 40TeV at 1×1(cm×cm) in 0.25GeV

Figure 5: Distributions of Mann-Whitney value U in 5, 10, 20, 40TeV energy collision for $\tau_{21}$ in different detector sizes. Cell Size in 20×20, 5×5, and 1×1(cm×cm) are shown here.

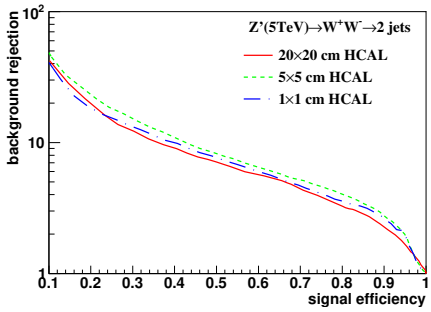


(a) 5 TeV rawhit cut at 0.25GeV compare with New2 Method

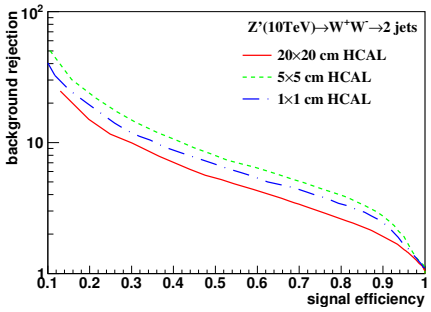


(b) 10 TeV rawhit cut at 0.25GeV compare with New2 Method

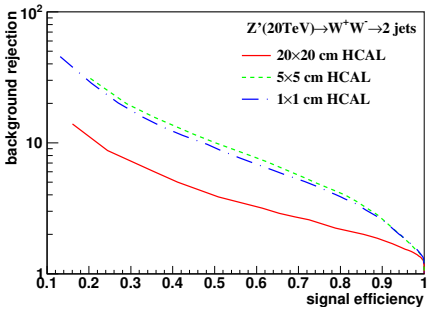


(c) 20 TeV rawhit cut at 0.25GeV compare with New2 Method

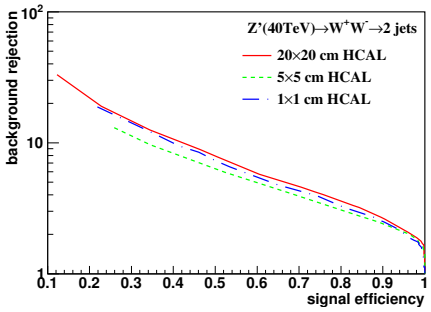


(d) 40 TeV rawhit cut at 0.25GeV compare with New2 Method

Figure 6: Signal efficiency versus background rejection rate using $\tau_{21}$.The energies of collision at (a)5, (b)10, (c)20, (d)40TeV are shown here. In each picture, the three ROC curves correspond to different detector sizes.

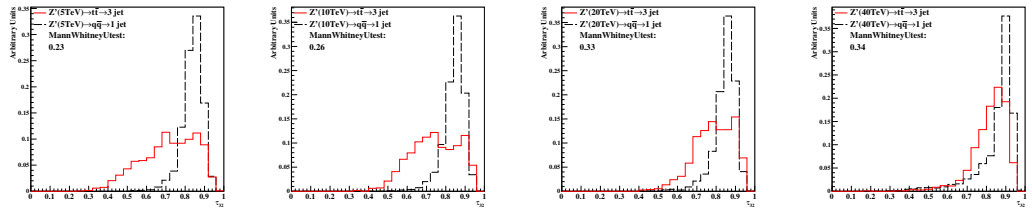


(a) 5TeV at 20×20(cm×cm) in 0.5GeV (b) 10TeV at 20×20(cm×cm) in 0.5GeV (c) 20TeV at 20×20(cm×cm) in 0.5GeV (d) 40TeV at 20×20(cm×cm) in 0.5GeV

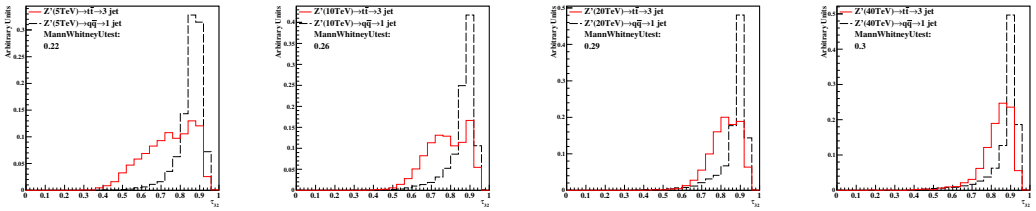


(e) 5TeV at 5×5(cm×cm) in 0.5GeV (f) 10TeV at 5×5(cm×cm) in 0.5GeV (g) 20TeV at 5×5(cm×cm) in 0.5GeV (h) 40TeV at 5×5(cm×cm) in 0.5GeV

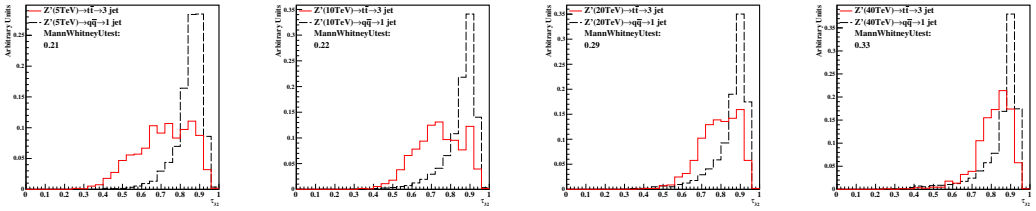


(i) 5TeV at 1×1(cm×cm) in 0.5GeV (j) 10TeV at 1×1(cm×cm) in 0.5GeV (k) 20TeV at 1×1(cm×cm) in 0.5GeV (l) 40TeV at 1×1(cm×cm) in 0.5GeV

Figure 7: Distributions of Mann-Whitney value U in 5, 10, 20 ,40TeV energy collision for $\tau_{32}$ in different detector sizes. Cell Size in 20×20, 5×5, and 1×1(cm×cm) are shown here.

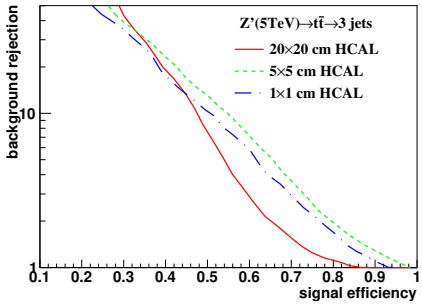


(a) 5 TeV rawhit cut at 0.5GeV compare with New2 Method

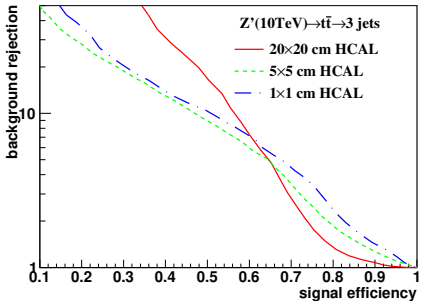


(b) 10 TeV rawhit cut at 0.5GeV compare with New2 Method

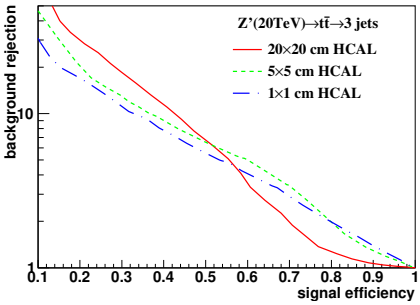


(c) 20 TeV rawhit cut at 0.5GeV compare with New2 Method

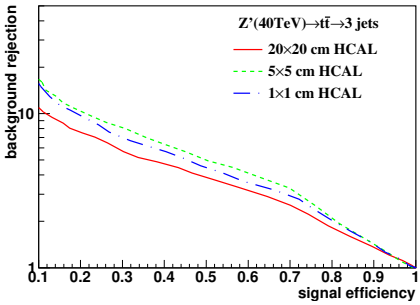


(d) 40 TeV rawhit cut at 0.5GeV compare with New2 Method

Figure 8: Signal efficiency versus background rejection rate using $\tau_{32}$.The energies of collision at (a)5, (b)10, (c)20, (d)40TeV are shown here. In each picture, the three ROC curves correspond to different detector sizes.

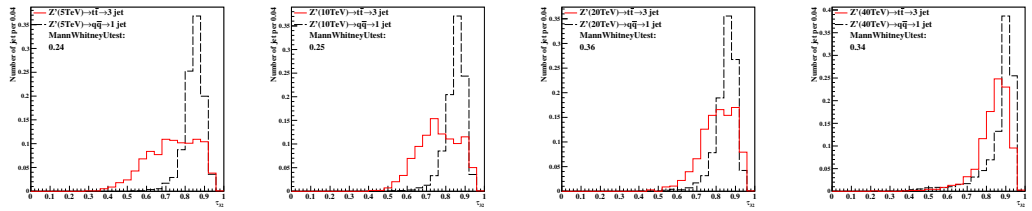


(a) 5TeV at 20×20(cm×cm) in 0.25GeV (b) 10TeV at 20×20(cm×cm) in 0.25GeV (c) 20TeV at 20×20(cm×cm) in 0.25GeV (d) 40TeV at 20×20(cm×cm) in 0.25GeV

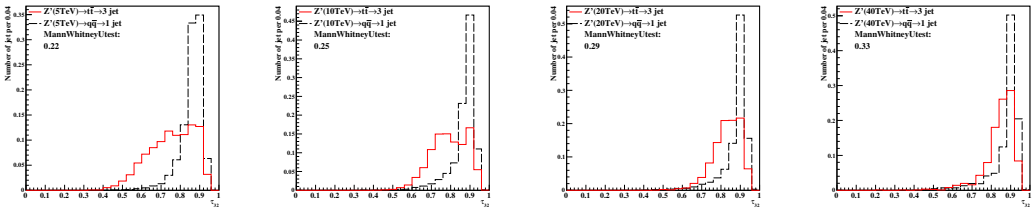


(e) 5TeV at 5×5(cm×cm) in 0.25GeV (f) 10TeV at 5×5(cm×cm) in 0.25GeV (g) 20TeV at 5×5(cm×cm) in 0.25GeV (h) 40TeV at 5×5(cm×cm) in 0.25GeV

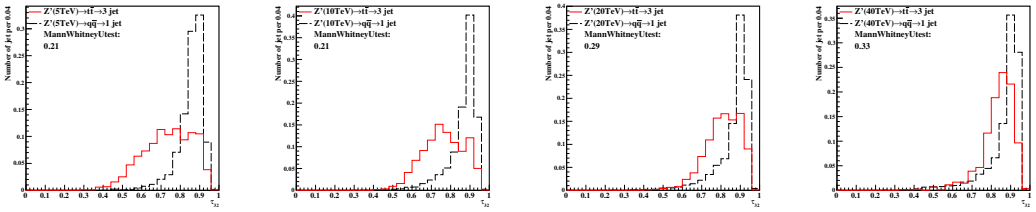


(i) 5TeV at 1×1(cm×cm) in 0.25GeV (j) 10TeV at 1×1(cm×cm) in 0.25GeV (k) 20TeV at 1×1(cm×cm) in 0.25GeV (l) 40TeV at 1×1(cm×cm) in 0.25GeV

Figure 9: Distributions of Mann-Whitney value U in 5, 10, 20 ,40TeV energy collision for $\tau_{32}$ in different detector sizes. Cell Size in 20×20, 5×5, and 1×1(cm×cm) are shown here.

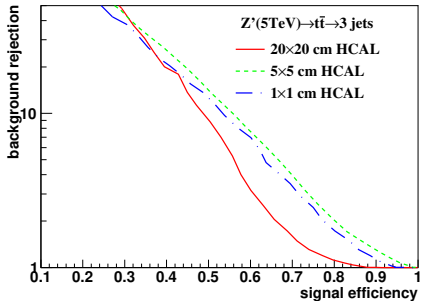


(a) 5 TeV rawhit cut at 0.25GeV compare with New2

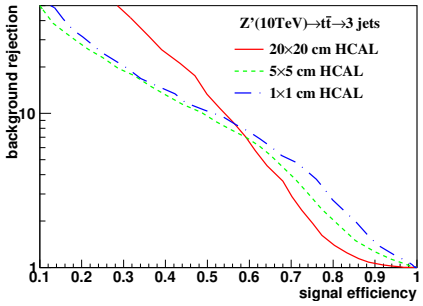


(b) 10 TeV rawhit cut at 0.25GeV compare with New2

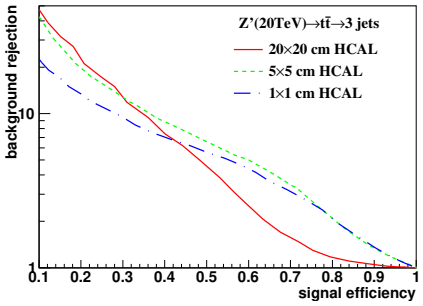


(c) 20 TeV rawhit cut at 0.25GeV compare with New2

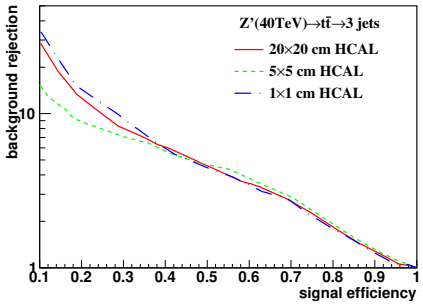


(d) 40 TeV rawhit cut at 0.25GeV compare with New2

Figure 10: Signal efficiency versus background rejection rate using $\tau_{32}$.The energies of collision at (a)5, (b)10, (c)20, (d)40TeV are shown here. In each picture, the three ROC curves correspond to different detector sizes.

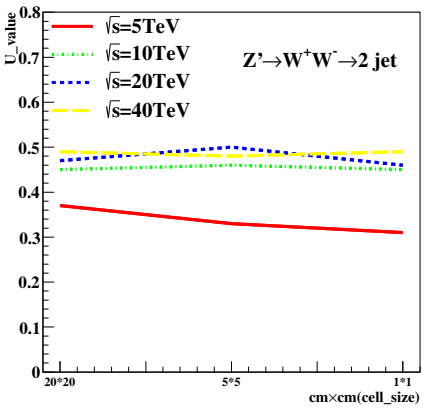


(a) $\tau_{21}$ in cluster

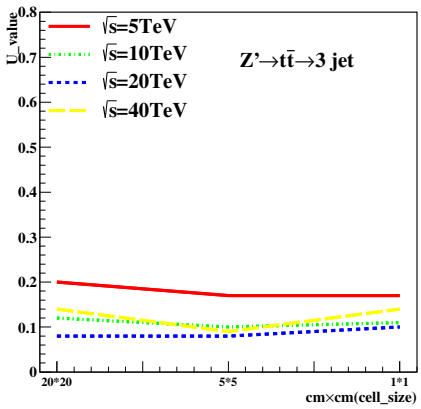


(b) $\tau_{32}$ in cluster

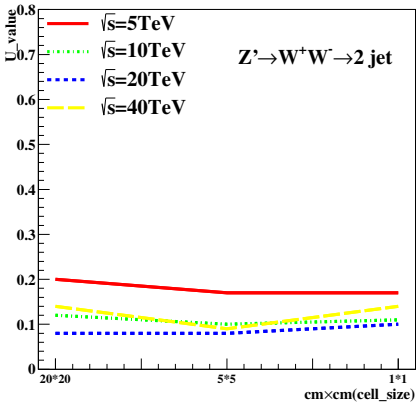


(c) $c_2^{(1)}$ in cluster

Figure 11: The Mann-Whitney U values for $\tau_{21}$,$\tau_{32}$ and $c_2^{(1)}$ reconstructed from calorimeter clusters at different collision energies correspond to different detector sizes in cluster. The energies of collision at 5, 10, 20, 40, 20, 40TeV are shown in each figure.

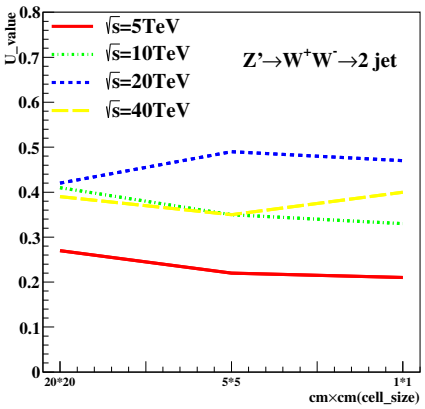


(a) $\tau_{21}$ rawhit cut at 0.5GeV

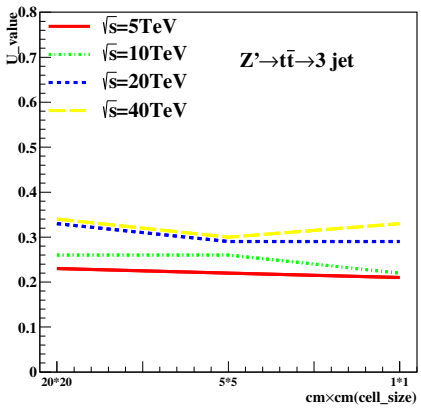


(b) $\tau_{32}$ rawhit cut at 0.5GeV

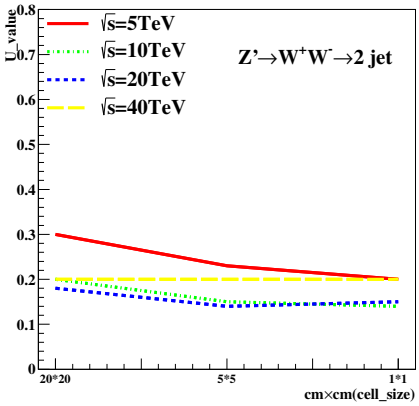


(c) $c_2^{(1)}$ rawhit cut at 0.5GeV

Figure 12: The Mann-Whitney U values for $\tau_{21}$,$\tau_{32}$ and $c_2^{(1)}$ reconstructed from calorimeter hit at 05GeV cut at different collision energies correspond to different detector sizes in rawhit cut at 05GeV. The energies of collision at 5, 10, 20, 40, 20, 40TeV are shown in each figure.

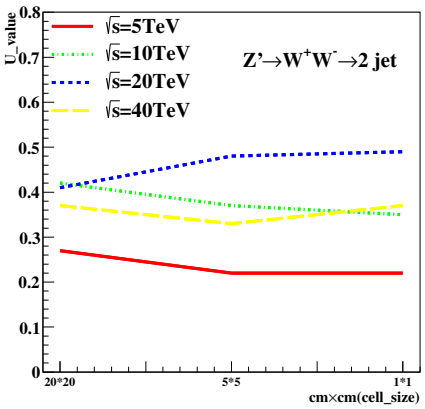


(a) $\tau_{21}$ rawhit cut at 0.25GeV

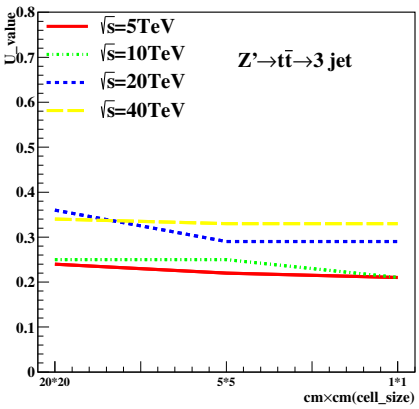


(b) $\tau_{32}$ rawhit cut at 0.25GeV

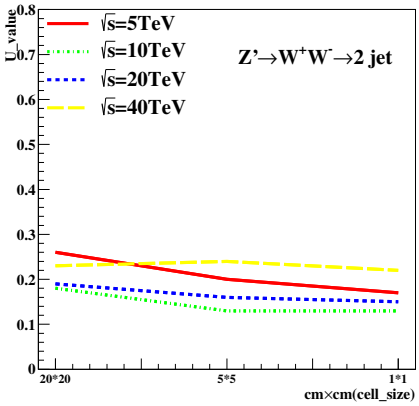


(c) $c_2^{(1)}$ rawhit cut at 0.25GeV

Figure 13: The Mann-Whitney U values for $\tau_{21}$,$\tau_{32}$ and $c_2^{(1)}$ reconstructed from calorimeter hit at 0.25GeV cut at different collision energies correspond to different detector sizes in cluster. The energies of collision at 5, 10, 20, 40, 20, 40TeV are shown in each figure.